THE JOURNAL OF PHYSICAL CHEMISTRY C

Article

CuSCN Nanowires as Electrodes for P-Type Quantum Dot Sensitized Solar Cells: Charge Transfer Dynamics and Alumina Passivation

Muhammad Tariq Sajjad, Jinhyung Park, Dorian Gaboriau, Jonathon R. Harwell, Fabrice Odobel, Peter Reiss, Ifor David William Samuel, and Dmitry Aldakov

J. Phys. Chem. C, **Just Accepted Manuscript** • DOI: 10.1021/acs.jpcc.7b12619 • Publication Date (Web): 13 Feb 2018

Just Accepted

ACS Publications

The Journal of Physical Chemistry C is published by the American Chemical Society. 1155 Sixteenth Street N.W., Washington, DC 20036

CuSCN Nanowires as Electrodes for p-Type Quantum Dot Sensitized Solar Cells: Charge Transfer Dynamics and Alumina Passivation

Muhammad T. Sajjad,[a] Jinhyung Park,[b] Dorian Gaboriau,[b] Jonathon R. Harwell,[a] Fabrice Odobel,[c] Peter Reiss,[b] Ifor D. W. Samuel,[a] Dmitry Aldakov[*,b]*

[a] *Organic Semiconductor Centre, SUPA, School of Physics and Astronomy, University of St Andrews, North Haugh, St Andrews, Fife, UK*

[b] *Univ. Grenoble Alpes, CNRS, CEA, INAC-SyMMES, 38000 Grenoble, France*

[c] *CEISAM, Chimie Et Interdisciplinarité, Synthèse, Analyse, Modélisation, CNRS, UMR CNRS 6230, UFR des Sciences et des Techniques; 2, rue de la Houssinière - BP 92208; 44322 Nantes Cedex 3, France*

Abstract

Quantum dot sensitized solar cells (QDSSCs) are a promising photovoltaic technology due to their low cost and simplicity of fabrication. Most QDSSCs have an n-type configuration with electron injection from QDs into TiO_2, which generally leads to unbalanced charge transport (slower hole transfer rate) limiting their efficiency and stability. We have previously demonstrated that p-type (inverted) QD sensitized cells have the potential to solve this problem.

Here we show for the first time that electrodeposited CuSCN nanowires can be used as a p-type nanostructured electrode for p-QDSSCs. We demonstrate their efficient sensitization by heavy metal free $CuInS_xSe_{2-x}$ quantum dots. Photophysical studies show efficient and fast hole injection from the excited QDs into the CuSCN nanowires. The transfer rate is strongly time dependent but the average rate of 2.5×10^9 s^{-1} is much faster than in previously studied sensitized systems based on NiO. Moreover, we have developed an original experiment allowing us to calculate independently the rates of charge injection and QD regeneration by the electrolyte and thus to determine which of these processes occurs first. The average QD regeneration rate (1.33×10^9 s^{-1}) is in the same range as the hole injection rate, resulting in an overall balanced charge separation process. To reduce recombination in the sensitized systems and improve their stability, the CuSCN nanowires were coated with thin conformal layers of Al_2O_3 using atomic layer deposition (ALD) and fully characterized by XPS and EDX. We demonstrate that the alumina layer protects the surface of CuSCN nanowires, reduces charge recombination and increases the overall charge transfer rate up to 1.5 times depending on the thickness of the deposited Al_2O_3 layer.

Introduction

An increasing number of energy-related applications rely on nanostructured wide band gap semiconductors. Due to their optical transparency and capacity to transport charges they find use in photovoltaics, photocatalysis, light-emitting devices, energy storage and other fields. The vast majority of semiconductors used are of n-type, such as TiO_2 and ZnO, which are responsible for the electron transport in various devices.[1–3] Transparent nanostructured p-type semiconductors

are much less studied primarily because of the scarcity of inorganic materials suitable for electronic applications compared to the n-type materials.[4] The main problems of p-type materials for sensitized photoelectrochemical devices are related to their low transparency and/or low conductivity.[5] A classic example is widely used nickel oxide, which can be made transparent, but with low conductivity. Its conductivity can be improved by doping by increasing the concentration of Ni(III) species, which in turn leads to the loss of transparency. In addition, many preparation methods suffer from a lack of control over the NiO stoichiometry, affecting the reproducibility. All factors together critically limit to date the performance of this material in optoelectronic devices.

Copper (I) thiocyanate, CuSCN, represents a promising alternative to NiO as an inorganic p-type material.[6] This molecular inorganic semiconductor has high transparency combined with decent hole-transporting properties: the hole mobility and the conductivity of the bulk material are 0.01-0.1 $cm^2 V^{-1} s^{-1}$ and 0.1-1 S/cm, respectively. Additionally, the stoichiometry of CuSCN can be better controlled than for many types of oxides, it can be relatively simply chemically modified[7,8] and its thermal stability is excellent.[9,10] Finally, CuSCN is inexpensive and easily adaptable for large area applications. Recently, thin films of CuSCN have been successfully used as hole-transporting layers in organic solar cells to replace traditionally used PEDOT:PSS material leading to improved performance in terms of power conversion efficiency and stability.[11–14] With the recent boom of hybrid perovskite photovoltaics, solution-deposited CuSCN has found several applications as hole-transporting and/or electron blocking layer. In these perovskite cells CuSCN replaced either spiro-OMeTAD in the case of n-i-p cells[9,15–19] or PEDOT:PSS in p-i-n ones,[20] outperforming the organic films even though some concerns about the stability of the cells at the interface level have been raised.[10] CuSCN was earlier used in dye-

sensitized solar cells (DSSCs) as a hole-transporting material in solid state cells in combination with sensitized TiO_2 or ZnO mesoporous electrodes,[7,21–23] and lately in nanostructured form as a p-type semiconductor scaffold in traditional liquid-junction cells.[24,25] While considerable progress has been achieved using CuSCN deposited on top of n-type semiconductors, its application as a hole acceptor from the adsorbed dye has met only limited success for several reasons: (i) the absence of an appropriate electrolyte system, as the iodide/triiodide redox couple is known to dissolve thiocyanates, while cobalt based electrolytes are less suitable because of faster recombination processes; (ii) the absence of appropriate dyes having suitable energy levels and capable of efficient and fast hole injection into CuSCN.[25] Another concern is the dye chemisorption: because of the soft Lewis acid character of the copper thiocyanate surface, traditional anchors, such as carboxylic and phosphonic acids developed for hard Lewis acidic TiO_2 electrodes, are not efficient. Therefore, alternative anchors for the dyes need to be developed for CuSCN.[24] Recently, using first-principles DFT and molecular dynamics calculations, a series of molecular anchors have been tested for the adsorption on CuSCN showing that most of the molecules have only moderate binding strength.[26]

Quantum dot sensitized solar cells (QDSSCs) appear as a promising photovoltaic technology because of the low production cost of quantum dots, their high absorption coefficients, and easily adjustable energy levels.[27] Moreover, the progress in the performance of QDSSCs is very fast with a current record power conversion efficiency of 12%, which is almost on par with their conventional dye-sensitized counterparts having a much longer history.[28] One of the factors still blocking further progress in this field is unbalanced charge transfer because of the slower hole regeneration compared to the fast electron injection into TiO_2 or similar materials.[29,30] With the goal of balancing both charge transfer processes and inspired by well-studied p-type DSSCs,[31]

inverted (or p-type) QDSSCs have been developed. They are based on the principle that faster hole injection into a p-type material combined with slower electron regeneration by the redox electrolyte can lead to similar transfer rates for both types of carriers. An additional advantage over organic dyes, especially when using ternary chalcopyrite nanocrystals,[32,33] comes from their naturally long-lived excited states allowing for more efficient charge injection and smaller recombination rates. Typically, NiO nanoparticles are used as mesoporous scaffold for the deposition of PbS, CdSe or chalcopyrite-type QDs.[34–37] The best cells, reaching 1.5% efficiency and reported by our group,[38] are based on eco-friendly $CuInS_xSe_{2-x}$ QDs. In this previous work we showed that the hole injection from QDs into NiO occurs on a similar timescale as electron injection into TiO_2 in n-type systems, confirming the general feasibility of sensitization of p-type materials by QDs. At the same time, because of the above-mentioned limitations of NiO, it is important to develop alternative nanostructured materials for p-QDSSCs. To date only a handful of working systems of this kind exists.[39,40] To the best of our knowledge, copper thiocyanate has never been used in QDSSCs, although a recent article demonstrated an efficient hole transfer from a thin layer of electrodeposited PbS to nanostructured CuSCN.[41]

In this work, we investigate electrodeposited CuSCN nanowires (NWs) as p-type semiconductors for sensitization with heavy metal-free $CuInS_xSe_{2-x}$ QDs for applications in p-QDSSCs. One important advantage of CuSCN NWs over thin films is their much higher hole concentration; an increase by a factor of 8 has been reported.[42] Previously, we have optimized the deposition of CuSCN NWs on various substrates,[43,44] investigated their structural properties[45] and successfully integrated them into organic photovoltaic devices.[11] Here, we present strategies for the efficient assembly of QDs on the surface of NWs and study the light harvesting properties of the sensitized electrodes. Time-resolved photoluminescence studies are used to estimate the

hole transfer rate between photoexcited $CuInS_xSe_{2-x}$ QDs and CuSCN NWs. In addition, for the first time the electron regeneration rate of the reduced QDs in the presence of a redox electrolyte has been calculated and the photophysical description of the complete system has been achieved. CuSCN NWs are sensitive to the pH of the medium and turned out to be incompatible with the polysulfide electrolyte commonly used in QDSSCs. An alternative electrolyte is proposed as well as a passivation strategy aiming at both NW protection against degradation and the suppression of charge recombination processes at the interface with the electrolyte. In the case of standard QDSSCs, passivation is typically achieved by coating thin layers of wide band gap ZnS or CdS onto the sensitized electrodes using successive ionic layer adsorption and reaction (SILAR). However, this method is not compatible with some materials.[46–48] Alternatively, atomic layer deposition (ALD) can be used to deposit highly conformal layers of metal oxides (e.g. Al_2O_3, HfO, TiO_2, ZnO) with tightly controllable thickness and composition.[49] This method has been previously used to coat TiO_2 and ZnO electrodes and indeed resulted in reduced recombination losses and improved QDSSC performance.[50–52] Here we present the deposition and X-ray photoelectron spectroscopy (XPS) analyses of thin Al_2O_3 layers on CuSCN NWs and study the influence of this passivation layer on the efficiency of the hole transfer.

Experimental section

Materials fabrication. CuSCN nanowires were fabricated on glass/ITO substrates by electrodeposition from aqueous solutions according to our previously published procedures.[11,43] Colloidal **$CuInS_xSe_{2-x}$:Zn^{2+} QDs** with 1-dodecanethiol/trioctylphosphine/ oleylamine ligands were synthesized similarly to previous works and used after the purification without the ligand exchange.[38,53]

Atomic layer deposition. ALD of Al_2O_3 thin films were carried out using trimethylaluminum (TMA) and H_2O as precursors in a Fiji200 reactor (Cambridge Nanotech). The deoxidized samples were placed in the deposition chamber under 100 °C, 10^{-2} Torr, argon purge gas and an automated recipe alternating 4 steps (0.06 s TMA, 30 s purge, 0.06 s H_2O and 30 s purge) was performed until the desired amount of cycles was attained. The deposition rate was estimated to be roughly around 0.9 Å/cycle, thus 1 and 3 nm thick layers were obtained using respectively 11 and 33 ALD cycles.

Characterisation. Air Photoemission Spectroscopy (APS) measurements were performed using a KP Technology APS03 Kelvin Probe setup. The sample was grounded and a gold tip was held ~100 microns above the sample. The sample was illuminated with monochromatic UV light in the energy range 4 – 6.5 eV and the resultant photoelectrons were collected by the tip, which was held at a constant +10V potential. The cube root of the number of photoelctrons was plotted against the energy of the incident photons, and the HOMO energy was calculated by extrapolating the straight line part of the graph to zero. The work function of the sample was measured before and after the APS measurement, using the APS03 setup in Kelvin Probe configuration, in order to ensure that the sample was not degraded by the high energy UV light. X-ray Photoelectron Spectroscopy (XPS) analyses were carried out with a Versa Probe II spectrometer (ULVAC-PHI) equipped with a monochromated Al Kα source (hν = 1486.6 eV). The core level peaks were recorded with constant pass energy of 23.3 eV. The XPS spectra were fitted with CasaXPS 2.3 software using Shirley background and a combination of Gaussian (70%) and Lorentzian (30%) distributions. Binding energies are referenced with respect to the adventitious carbon (C 1s BE = 284.6 eV). Scanning electron microscopy (SEM) images were acquired with a ZEISS Ultra 55+ Electron Microscope equipped with EDX detector.

Solar cells fabrication. QD sensitized solar cells were prepared using various electrolytes: polysulfide (1.0 M Na_2S, 1.0 M S, 0.1 M NaOH in water), cobalt (0.1 M $[Co^{2+}(dtb\text{-}bpy)_3](PF_6)_2$, 0.1 M $[Co^{3+}(dtb\text{-}bpy)_3](PF_6)_3$ where dtb-bpy is 4,4′ -diterbutyl-2,2′-bipyridine, and 0.1 M $LiClO_4$ in propylene carbonate)[35], ferrocyanide/ferricyanide (0.01 $K_3Fe(CN)_6$, 0.2 M $K_4Fe(CN)_6$ in water).[54] As a counter electrode for polysulfide electrolytes, brass plates was activated in 1.0 M HCl solution at 85°C for 30 min followed by rinsing with water. For cobalt and ferrocyanide electrolytes, platinum counter-electrodes (Solaronix SA, Switzerland) were used. Sensitized CuSCN NWs grown on glass/ITO substrates were assembled with counter-electrodes using parafilm spacers and the electrolyte was injected in the cavity. The device active area was 0.6 x 0.6 cm (that is 0.36 cm^2). The solar cells were measured using a Keithley 2400 unit and 1000 Wm^{-2} air-mass 1.5G simulated solar light generated by a Newport class AAA solar simulator. A calibrated monocrystalline silicon solar cell (P/N 91150V from Oriel) was used as a reference.

Photophysical studies. Varian Cary 300 UV-Vis spectrophotometer was used to measure the absorption spectra of samples and Edinburgh Photonics Instrument FLS980 was used to measure the photoluminescence decays. For lifetime measurements, the samples were excited with a 470 nm PicoQuant picosecond pulsed laser and PL was measured at 770 nm using time correlated single photon counting (TCSPC). The instrument has a time resolution of ~200 ps.

Results and Discussion

Deposition of QDs onto CuSCN nanowires. CuSCN NWs with 1 μm length and 100 nm diameter have been fabricated by electrodeposition from aqueous solutions to yield uniform layers on ITO-coated glass substrates (Figure 1). It is worth noting that it is generally challenging

to obtain an image of CuSCN nanowires by electron microscopy as the probing beam rapidly modifies the morphology of the NW arrays rendering the aspect ratio of nanowires progressively lower and ultimately resulting in tapered structures. Deposition of a thin layer of a conducting material such as carbon or Pt is thus necessary to get high quality images.

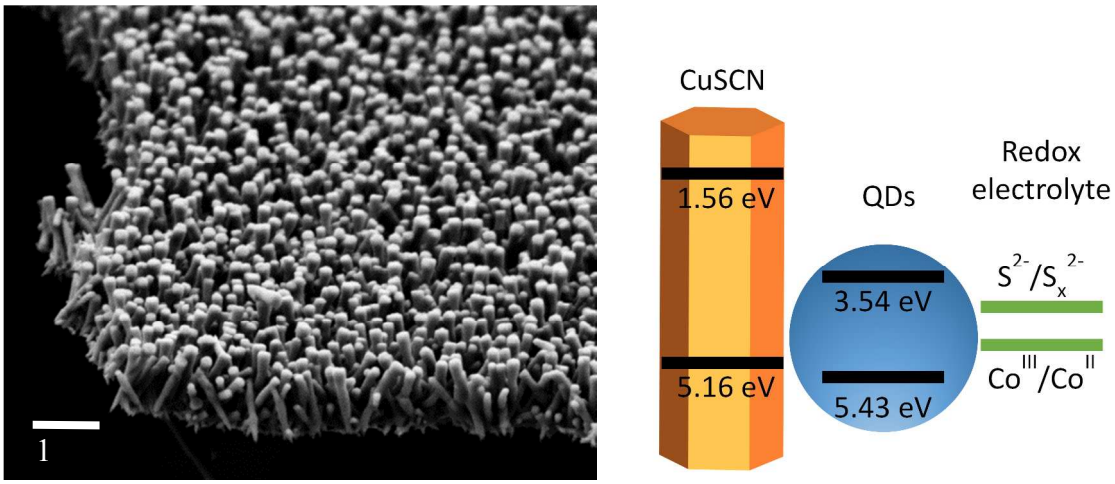

Figure 1. Scanning electron microscope (SEM) image of CuSCN nanowires array coated with Pt (left). Hypothetical energy level alignment (right).

While the electronic properties, such as energy level positions, charge mobility and conductivity of spin- or dip-coated films of commercial CuSCN are relatively well studied,[55] little is known about the nanowire form of this material having completely different crystallinity and morphology. The band gap value of 3.6 eV, having an indirect contribution in the case of the NWs, is close to that of bulk CuSCN.[11,45] The absolute position of the valence band (VB) has been determined by ambient pressure photoemission spectroscopy (APS), by investigating a plot of cube root of the photoelectron yield as a function of photon energy for a CuSCN layer on ITO electrodes. The intercept and fit of the curve allowed calculating the position of the VB at -5.16 ± 0.10 eV, while the work function (WF) is situated at roughly the same value: -5.17 ± 0.01 eV (see Fig. S1). For comparison, the VB and the WF of flat electrodeposited CuSCN films were

measured under the same conditions at -4.81 eV and -4.85 eV, respectively. In a recent work the WF of spin-coated commercial CuSCN films was determined as -5.35 ± 0.11 eV.[56]

Alloyed $CuInS_xSe_{2-x}$ QDs have been used as photosensitizers in this work. Taking into account the levels of their VB and conduction bands recently determined by differential pulse voltammetry,[38] one can establish the scheme of the energy level alignment of the $CuSCN/CuInS_xSe_{2-x}$ QDs junction (Figure 1). The proposed alignment is beneficial for hole injection from the VB of the excited QDs into the VB of CuSCN with an energy difference of 0.27 eV acting as an efficient driving force. Moreover, the deep-lying VB of the CuSCN NWs gives the possibility of attaining high open-circuit voltages (V_{OC}) in solar cells. In p-type QDSSCs the V_{OC} is defined by the difference of the VB of the p-type semiconductor and the redox potential of the electrolyte. At the same time, the wide band gap of CuSCN is essential for limiting its direct light absorption and avoiding QD quenching.

By using molecular linkers higher QD loading on the nanostructured electrodes can be achieved because of the increased deposition density due to specific binding. One of the most efficient linkers developed for TiO_2 sensitized by various QDs are mercaptocarboxylic acids, such as 3-mercaptopropionic acid (MPA). According to the Pearson acid base concept, the carboxylate group, having hard acid character, will preferably bind to Ti^{+4} sites, while the soft thiol group will selectively bind to the soft base cations of the QDs. Although working well for TiO_2, this concept has previously proved incompatible with ZnO nanowires[57] and less efficient for NiO.[38] In the present case, the functionalization of CuSCN nanowires with MPA to improve the QD loading turned out to be counterproductive because of the gradual dissolution of the NWs in the acidic medium. Interestingly, the dissolution proceeds through flower-like structures of high surface area and the diffraction peaks corresponding to vertically oriented CuSCN NWs

(JCPDS 04-017-0744) are strongly diminished giving rise to others, probably related to the copper sulfides, as observed by the XRD (Figure 2).

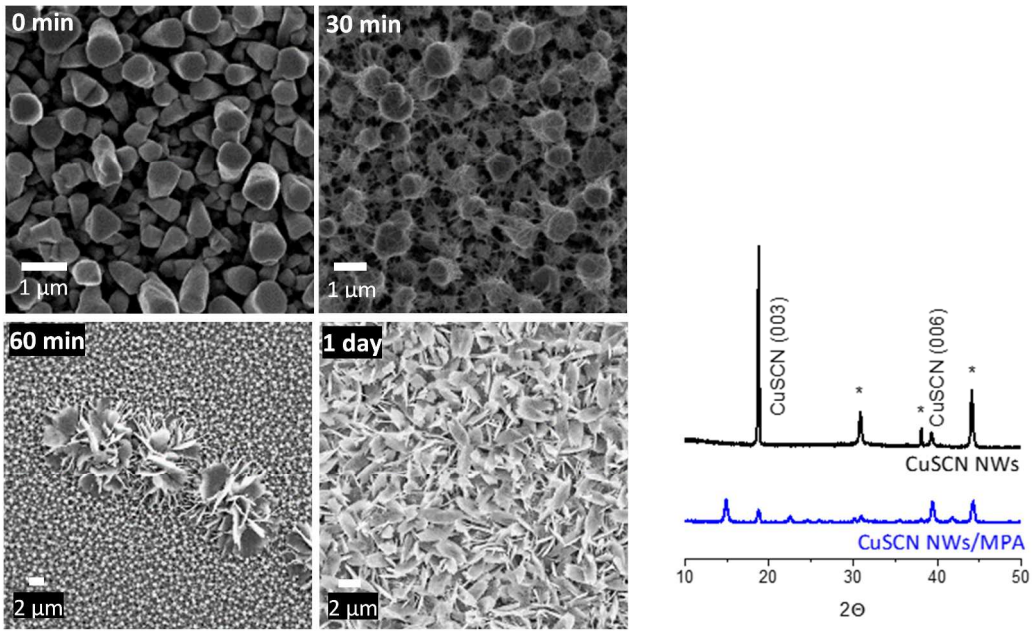

Figure 2. SEM (left) and powder XRD diffractograms (right) showing the influence of 3-mercaptopropionic acid (MPA) treatment (1 M in water) on the morphology of CuSCN nanowires. * - ITO substrate peaks.

As a consequence of the high sensitivity of CuSCN towards the tested bifunctional linkers, a specific binding route to deposit QDs on the NWs has been abandoned in favor of direct adsorption, which has been shown to be efficient in a range of systems.[38,47,58] Figure 3 shows the absorption spectra of the QD sensitized CuSCN NWs as a function of the deposition time. Because of its wide band gap CuSCN is not expected to absorb light above 350 nm. Therefore the absorption of the uncoated nanowires observed at larger wavelengths is explained by light scattering due to the high diffusivity of the array. The absorption of the NWs in the visible range greatly increases upon QD deposition. Assuming that the absorption values are proportional to

the QD loading onto the nanowires, we can deduce that the loading gradually increases with time.

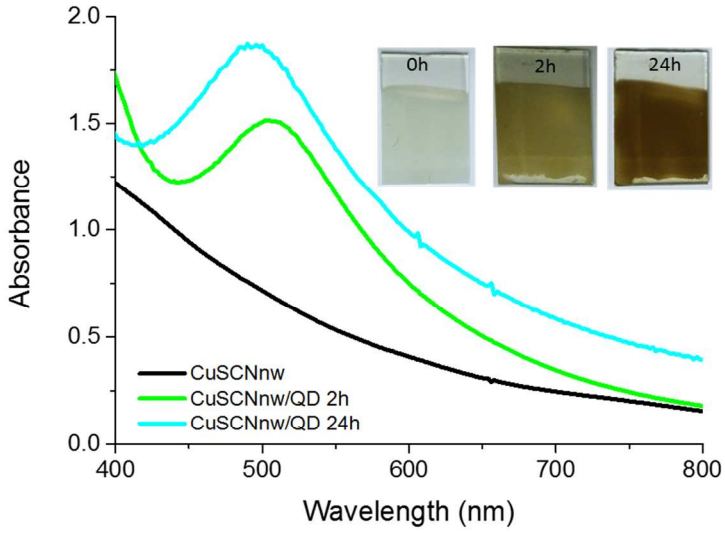

Figure 3. Absorption spectra of CuSCN NWs sensitized with $CuInS_xSe_{2-x}$ QDs at different sensitization times.

Hole and electron transfer studies of the assemblies. In order to estimate the hole and electron transfer efficiency, time-resolved photophysical studies have been carried out taking the photoluminescence (PL) peak of QDs at around 770 nm as the indicator. First, the PL decay of a thin film of QDs was measured in the absence of electron or hole accepting materials on a glass substrate. Then, with the goal to determine the hole transfer rate, the same experiment was repeated for QDs deposited on CuSCN NWs. However, to get a complete picture of the charge separation in systems used for the photovoltaic conversion, also electron transfer studies have to be conducted. It is of prime importance to understand which of both processes takes place first to identify the rate-limiting one to be able to optimize the system. Their rates should be compared

in conditions close to those occurring in real solar cells to be able to elucidate and optimize the full mechanism of charge separation. Only a handful of studies have been focused so far on this problem.[29,59,60] We have designed an experiment allowing the estimation of the electron extraction in the absence of a hole quencher: a simple cell was constructed with a QD film on glass in contact with a redox electrolyte, mimicking the configuration in a QDSSC. Upon photo-excitation the charges are extracted by the electrolyte allowing the determination of the rate of the other electrode half-reaction. Finally, the combined rate constant of hole and electron transfer of the complete system was determined by QD lifetime measurements on sensitized CuSCN electrodes in the presence of the electrolyte.

Inspired by the state of the art of QDSSCs we initially intended to use the widely applied polysulfide electrolyte as a redox shuttle. However, it turned out that it was not compatible with the CuSCN nanowires. The elevated basicity (pH=11-12) coupled with the presence of active S^{2-} species in the polysulfide electrolyte led to the rapid corrosion of the nanowires (see Fig. S6) rendering further studies impossible. Consequently, we have selected an alternative organic electrolyte based on the Co^{II}/Co^{III} redox couple ((tris(4,4'-ditert-butyl-2,2'-bipyridine) cobalt(III/II)).[35,61] This system is more inert and gives also the possibility to access higher V_{OC} values in solar cells compared to polysulfides.[62] The use of cobalt electrolyte significantly increased the stability of the nanowires.

The QD PL decays of the different systems are shown in Figure 4a. As expected, the QDs decay is faster in the presence of a quencher (CuSCN, electrolyte or combination of both) than on glass due to charge transfer processes competing with radiative recombination. The PL quenching rate is determined by taking the natural logarithm of the ratio of the PL decay of the QDs on CuSCN to their decay on glass (see Fig. S5 and Eq. 1). This method has proven to be

well suited for emitters, which do not show monoexponential decay, which is the case for ternary metal chalcogenide NCs.[57] While this procedure would give a flat line in the absence of quenching (no charge transfer) and a line of a constant slope in the case of constant transfer rate, our curves show non-linear behavior. This suggests a strongly time-dependent charge transfer similar to that observed for QDs on NiO, TiO_2 or ZnO.[38,57] The time-dependent rate constants were calculated through differentiation of the natural logarithm of the PL ratio using equation 1:

$$k_{CT}(t) = -\frac{d}{dt}\left(log_e\left(\frac{PL\ of\ QDs\ with\ quencher}{PL\ of\ QDs\ on\ glass}\right)\right) \quad (1)$$

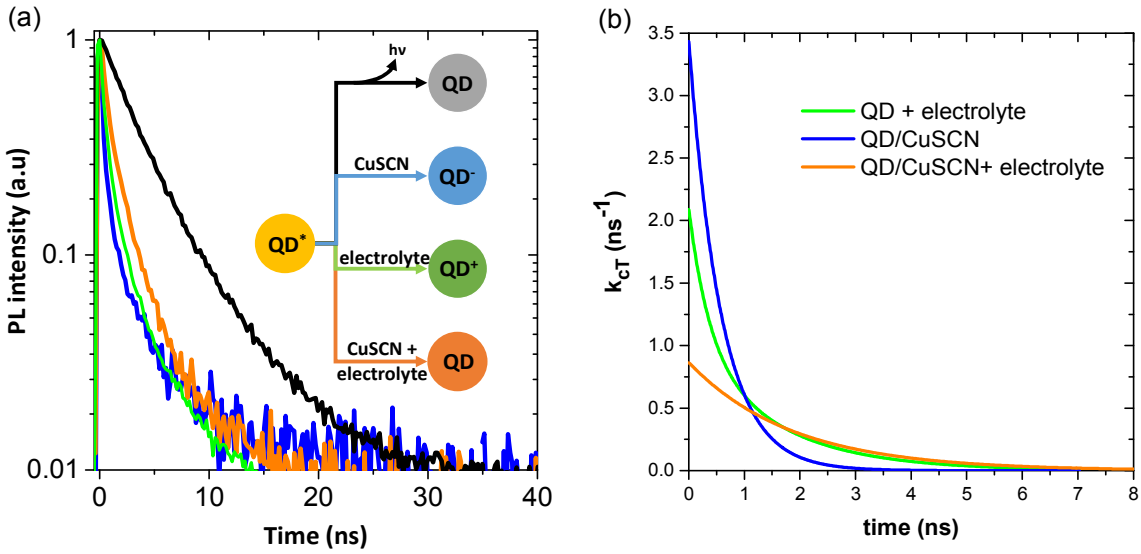

Figure 4: (a) PL decay profiles of $CuInS_xSe_{2-x}$ QDs in the absence and presence of electrolyte. The black curve is the PL decay of QDs on glass, the blue curve is the decay of QDs deposited on CuSCN, the green curve is the decay of QDs on glass in the presence of electrolyte and the orange curve is the decay of QDs in the presence of electrolyte and CuSCN. Inset: Scheme of deactivation pathways in various systems. (b) Rate constants of charge transfer determined through differentiation of the natural logarithm of the PL decay ratios.

The charge transfer rates (Figure 4b) were determined by fitting the natural logarithm of the PL decay ratios with three exponentials before differentiation. The obtained curves clearly show that the charge transfer rates are strongly time dependent. It can be seen from Figure 4b that in the first nanosecond, the transfer from QDs deposited on CuSCN is faster than that from QDs on glass in the presence of electrolyte, which is in turn faster than QDs the presence of electrolyte and CuSCN. For comparison, we determine the average charge transfer rate by integrating the rates over the times for the PL to fall to 1/e of its initial value using equation 2:

$$\langle k_{CT} \rangle = \frac{1}{\tau_{1/e}} \int_0^{\tau_{1/e}} k_{CT}(t)\, dt \qquad (2)$$

The resulting values (Table 1) show that the hole transfer from QDs to CuSCN is almost twice as fast as the charge extraction of the excited QDs by the redox electrolyte, occurring on a timescale of 0.4 ns and 0.75 ns, respectively. We assume that the PL decay rate constant corresponds to the hole transfer (k_{HT}) in the case of the CuSCN/QD system and to the charge extraction (k_{ET}) in the case of QDs in the presence of the redox electrolyte. However, at this QD-electrolyte interface we cannot fully exclude that quenching also occurs *via* hole extraction from the reduced form of the redox mediator (cf. energy level alignment in Fig. 1). For the complete systems with both electron and hole quenchers, the determined constant has arbitrary character and reflects the averaged influence of both interfaces on the QD PL decay. Noteworthy, the obtained average hole transfer rate value (2.5×10^9 s^{-1}) is almost 50 times higher than in previously studied NiO based systems, confirming the benefits of using CuSCN nanowires as hole acceptor.[38] Furthermore, k_{ET} is 10 times higher than the electron injection into n-type materials in QD assemblies.

Table 1. Charge transfer rate constants averaged over the first 1/e of the fluorescence decay in the different systems studied

	QD/CuSCN	QD + electrolyte	QD/CuSCN + electrolyte
k_{CT} (10^9 s^{-1})	2.50	1.33	0.66

An important criterion for the efficient functioning of the sensitized solar cells is balanced charge transfer. One of the reasons is that the QDs remain charged between the event of charge (electron or hole) injection occurring first and the consequent opposite charge injection (or regeneration) to regain neutrality. If the injection/regeneration rate of one type of charge carriers is much faster than that of the opposite one, charges will accumulate in the QDs.[60] This can lead to increased recombination or to lower stability, as charged QDs are more reactive. In the case of n-type QDSSCs hole regeneration can be 2-3 orders of magnitude slower than initial electron injection, which may lead to undesired photocorrosion.[29] In the studied CuSCN/QD/electrolyte system the hole and electron extraction rates are comparable, resulting in balanced charge transfer, which is beneficial for the overall performance and stability of the system. The lower charge transfer rate in the complete systems with electrolyte compared to the QDs on nanowires alone may indicate some modification of the CuSCN surface in the presence of the cobalt electrolyte leading to a lower electronic coupling with the QDs.

To validate the approach of CuSCN sensitization by $CuInS_xSe_{2-x}$ QDs we have constructed p-QDSSCs using these systems. The cells using polysulfide electrolyte and vulcanized brass as counter-electrode developed a J_{SC} of 0.59±0.08 mA/cm² with a modest open-circuit voltage V_{OC} of 53±8 mV. For comparison, $CuInS_2$ QDs without Se additive resulted in a V_{OC} of 159±43 mV. One of the possible reasons of the poor solar cell performance is the aforementioned low stability

of the CuSCN NWs in alkaline solutions of polysulfide electrolyte. On the other hand, using the cobalt-based electrolyte, which is expected to be less corrosive, similar performances were obtained (J_{SC}: 0.54 mA/cm², V_{OC}: 40 mV). An important limiting factor here is the potential of the redox couple in the Co^{II}/Co^{III} electrolyte: the maximum V_{OC} of p-QDSSCs is defined by the difference between the electrolyte redox potential and the VB level of p-type semiconductor. Because of losses due to the series resistance and recombination processes, even for the best reported p-QDSSCs a voltage drop of about 50% (500 mV) has been reported.[38] While with the polysulfide electrolyte this potential difference reaches 1.06 eV (the VB of CuSCN NWs is at -5.16 eV vs. vacuum and the redox potential of polysulfide is -4.10 eV), it is limited to 0.27 eV for the organic cobalt electrolyte because of its lower lying redox potential (-4.89 eV) (Fig. 1), which may critically limit the theoretically attainable V_{OC} in such systems. These issues need to be addressed in future work; despite these shortcomings, our results demonstrate the first successful sensitization of CuSCN NWs by QDs.

Al_2O_3 coating of CuSCN nanowires. With the goal to protect the NWs against corrosion by the electrolyte and to passivate their surface to reduce charge recombination, thin layers of Al_2O_3 of varying thickness were deposited by ALD on their surface. The ALD technique has the advantage of depositing thin, very conformal coatings of precisely controlled thickness and composition. As expected, the stability of the NWs in various electrolytes was improved after such coating.

The elemental composition of the NWs coated by 1 nm of Al_2O_3 was studied by EDX (Table 2) revealing that the CuSCN material remains intact and close to the nominal stoichiometry with a small contribution of aluminum in the overall composition.

Table 2. Chemical composition of CuSCN nanowires coated by 1 nm of Al_2O_3 determined by EDX.

	Cu	**S**	**C**	**N**	**Al**	**O**
Composition, %	27.5±4.6	19.8±2.0	28.2±2.0	19.9±0.1	0.7±0.2	3.3±0.5

The surface of the coated nanowires is the key interface for the electronic processes such as charge transfer and recombination. One of the essential methods allowing to probe the surface composition is X-ray photoelectron spectroscopy (XPS). In the survey spectrum of CuSCN / Al_2O_3 nanowires the peaks of all expected elements are observable (Figure 5). The aluminum 2p peaks at 74.4 eV are clearly visible, while the Cu 2p, S 2p and N 1s signals are undoubtedly attenuated upon deposition of Al_2O_3 layers of increased thickness (see Fig. S3) because the average probing depth of the surfaces of XPS beam is about 3 nm. This attenuation coupled with a slight shift of the peaks position confirms the conformal deposition of Al_2O_3 layer onto the CuSCN nanowires (see also Fig. S7).[63] The chemical structure of the NWs after the coating revealed by the XPS remains essentially intact with respect to the previously studied uncoated nanowires.[45] Elemental composition found by XPS is considerably different from that determined by the EDX analysis: the ratio [Cu]:[Al] is 1:1.44 and 1:5.59 for 1 and 3 nm coating, respectively, while the ratio measured by EDX is much lower, in the order of 1:0.03. This difference is explained by the surface sensitivity of XPS technique, while the EDX probes the full volume of the nanowires: a much higher contents of Al at the surface confirms that Al_2O_3 material is not incorporated into the CuSCN NWs during the deposition and occurs essentially as a surface layer.

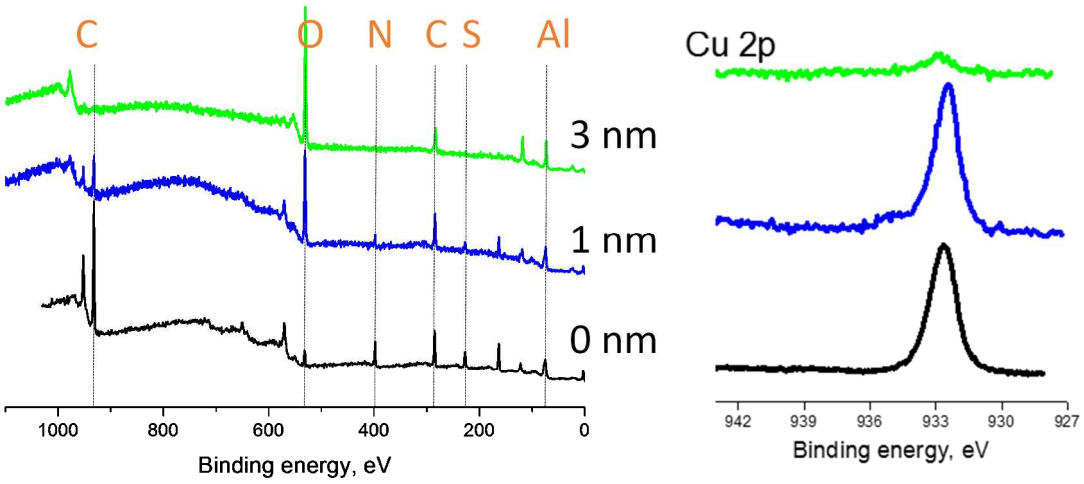

Figure 5. XPS spectra of CuSCN NWs coated with Al_2O_3: survey spectra (left), Cu 2p high resolution region (right).

The effect of the deposited Al_2O_3 layer on the charge transfer processes was studied by time-resolved PL spectroscopy. First, we investigated the PL decays of sensitized CuSCN films in the presence of 1 or 3 nm Al_2O_3 layers in air (Figure 6). For comparison, the PL decay in the absence of the Al_2O_3 layer was also plotted (black line). The hole transfer rates were determined using eqs. 1 and 2 and the obtained average values are given in Table 3. Upon the deposition of the passivation barrier the hole transfer becomes slower, dropping almost by a factor of 3 for an alumina coating of 3 nm, which can be explained in terms of the potential barrier introduced by this wide band gap material. Charge transfer from QDs to CuSCN through the Al_2O_3 layer is not favorable kinetically albeit remains possible *via* electron tunneling. With the increasing thickness of the insulator the tunneling expectedly becomes less efficient.

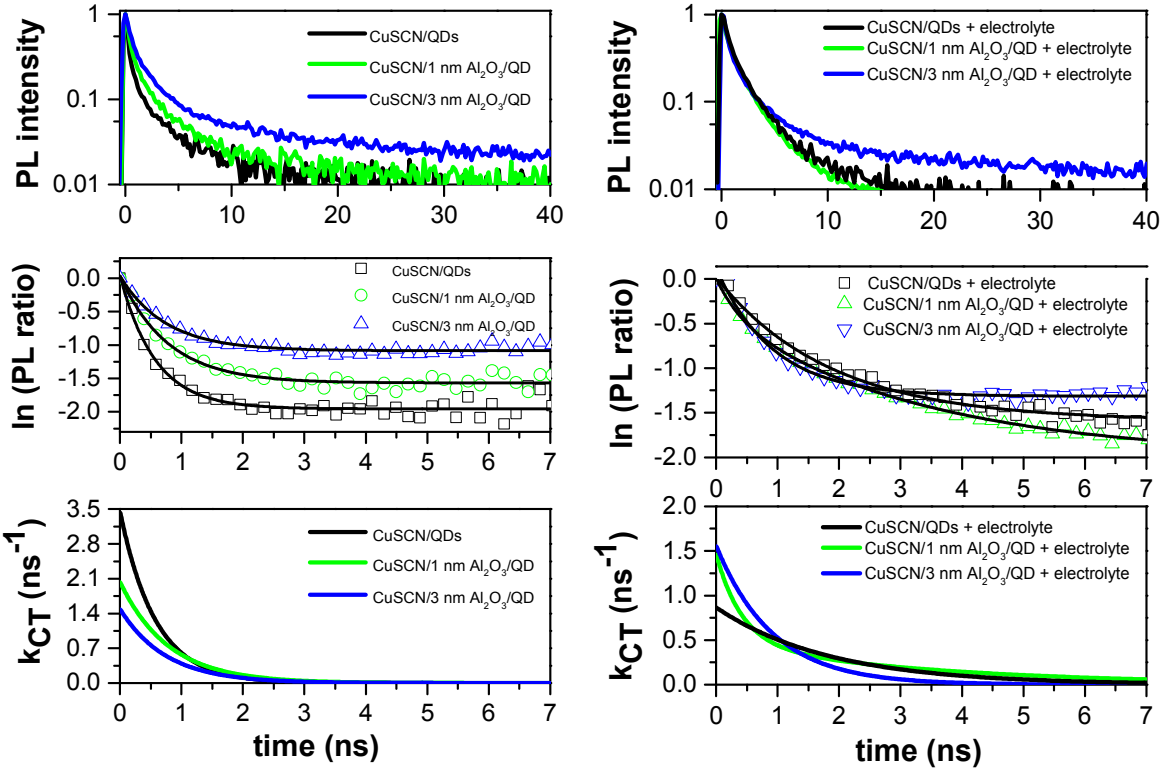

Figure 6. Photophysical studies of CuSCN/QD systems as a function of Al_2O_3 thickness in air (left panel) and in the presence of electrolyte (right panel).

By adding the redox electrolyte to the system the effect of the deposited Al_2O_3 layer on the overall charge transfer (in actual solar cell conditions) has also been investigated. The results are shown in Figure 6 (right panel). The obtained average values of charge transfer (combination of both electron and hole transfer) are given in Table 3 and follow the trend observed previously for the uncoated nanowires: the charge transfer processes occur at similar rates on the CuSCN quencher and in the presence of the electrolyte. Interestingly, in the presence of the electrolyte the average charge transfer rates actually become faster with increasing Al_2O_3 layer thickness. This behavior confirms our interpretation of the lower transfer rate in the complete systems CuSCN/QD/electrolyte (Table 1). We assume that the cobalt electrolyte slightly modifies chemical and thus electronic properties of the CuSCN surface (e.g. by shifting its Fermi level)

leading to a less efficient charge injection from the QDs into CuSCN. Similar behavior has been previously observed in the case of NiO sensitized with organic dyes in the presence of iodide electrolyte.[64] However, when the surface of the NWs is coated with the alumina layers of increasing thicknesses, the mentioned effects of the electrolyte on the CuSCN NWs are becoming weaker and consequently the charge transfer becomes faster. In other words, despite the relative slowing of the charge injection from the QDs into CuSCN, in the complete systems with the electrolyte Al_2O_3 plays the role of a protecting barrier leading to an overall improvement of the charge transfer process.

Table 3. Charge transfer rates averaged over the first 1/e of the fluorescence decay in the systems based on QDs on CuSCN and on CuSCN/Al_2O_3

k_{CT} (10^9 s^{-1})	No Al_2O_3	1 nm Al_2O_3	3 nm Al_2O_3
In air	2.50	1.43	0.83
In electrolyte	0.66	0.79	0.99

Solar cells using QD-sensitized nanowires with a 3 nm Al_2O_3 overlayer demonstrated modest photovoltaic performance with a V_{OC} of 30±15 mV and a photocurrent density of 0.27±0.22 mA/cm², probably limited again by electrolyte incompatibility issues. An alternative ferri/ferrocyanide electrolyte[54] was also tested, however, its deep lying redox potential (-5.0 eV) and corrosivity towards the NWs render it unsuitable for such type of solar cells. These results show that the high potential of CuSCN NWs for use as photoelectrodes in QD sensitized solar cells currently remains unexploited because of the absence of suitable redox electrolytes. The quest for appropriate redox couples to take full advantage of this promising material is

underway. Another viable strategy allowing to benefit from promising properties of CuSCN NWs for sensitized solar cells is to use solid electrolytes as electron transport materials.[65]

Conclusions

Heavy metal free $CuInS_xSe_{2-x}$ QDs have been successfully used to photosensitize CuSCN NWs. The established energy diagram shows optimal alignment of the energy levels for efficient hole injection from the QDs into CuSCN and regeneration with two electrolytes studied (polysulfide and organic cobalt complex based redox systems) is also possible. Photophysical studies confirm efficient hole injection with a strongly time-dependent rate. When averaged over the first 1/e of decay, an average rate of 2.5×10^9 s^{-1} is obtained, which is faster than the hole injection rate into NiO with the same QDs. For the first time we have also studied the regeneration of the $CuInS_xSe_{2-x}$ QDs in presence of the electrolyte and absence of the CuSCN NWs. The resulting average charge transfer rate of the electrolyte is 1.33×10^9 s^{-1} showing that hole injection into CuSCN takes place at a faster rate than electron transfer to the redox mediator. However, both rates are of the same order of magnitude, enabling overall balanced charge separation. To reduce recombination processes in the sensitized systems, Al_2O_3 coating of the CuSCN NWs has been realized using the ALD method. As expected, the presence of an insulating barrier on the NW surface reduces the hole injection rate from QDs to CuSCN, measured in the absence of electrolyte. To the contrary, in the presence of the electrolyte the charge separation dynamics approaches the case of QD/electrolyte systems (without CuSCN) with increasing alumina thickness. Concluding, our results demonstrate the appealing fundamental features of QD-sensitized CuSCN NWs for use in photoelectrochemical devices. To

exploit their full potential in QDSSCs, the development of non-corrosive electrolyte systems showing appropriate redox levels is required.

ASSOCIATED CONTENT

Supporting Information: SEM images of CuSCN NWs, EDX and XPS spectra, PL decay profiles, J-V curves. This material is available free of charge via the Internet at http://pubs.acs.org.

AUTHOR INFORMATION

Corresponding Author

*E-mail: dmitry.aldakov@cea.fr

Acknowledgements

The work was supported by the Agence Nationale de la Recherche, project QuePhélec (ANR-13-BS10-0011-01). We also acknowledge support from the European Research Council (grant number 321305) and the EPSRC (grant numbers EP/L017008/1 and EP/M506631/1). IDWS is a Royal Society Wolfson Research Merit award holder. The authors would like to thank Dr. Stéphanie Pouget (CEA/INAC/MEM/SGX) for help with the XRD and Dr. Mahfoudh Raissi (Univ. Nantes/CEISAM) for the photovoltaic measurements.

REFERENCES

(1) Yu, X.; Marks, T. J.; Facchetti, A. Metal Oxides for Optoelectronic Applications. *Nat. Mater.* **2016**, *15* (4), 383–396.

(2) Sun, J.-K.; Jiang, Y.; Zhong, X.; Hu, J.-S.; Wan, L.-J. Three-Dimensional Nanostructured Electrodes for Efficient Quantum-Dot-Sensitized Solar Cells. *Nano Energy* **2016**, *32*, 130–156.

(3) Chen, X.; Mao, S. S. Titanium Dioxide Nanomaterials: Synthesis, Properties, Modifications, and Applications. *Chem. Rev.* **2007**, *107*, 2891–2959.

(4) Thomas, S. R.; Pattanasattayavong, P.; Anthopoulos, T. D. Solution-Processable Metal Oxide Semiconductors for Thin-Film Transistor Applications. *Chem. Soc. Rev.* **2013**, *42* (16), 6910–6923.

(5) Odobel, F.; Pellegrin, Y. Recent Advances in the Sensitization of Wide-Band-Gap Nanostructured P-Type Semiconductors. Photovoltaic and Photocatalytic Applications. *J. Phys. Chem. Lett.* **2013**, *4* (15), 2551–2564.

(6) Wijeyasinghe, N.; Anthopoulos, T. D. Copper(I) Thiocyanate (CuSCN) as a Hole-Transport Material for Large-Area Opto/electronics. *Semicond. Sci. Technol.* **2015**, *30* (10), 104002.

(7) Premalal, E. V. A.; Kumara, G. R. R. A.; Rajapakse, R. M. G.; Shimomura, M.; Murakami, K.; Konno, A. Tuning Chemistry of CuSCN to Enhance the Performance of TiO2/N719/CuSCN All-Solid-State Dye-Sensitized Solar Cell. *Chem. Commun.* **2010**, *46* (19), 3360–3362.

(8) Miller, K. M.; McCullough, S. M.; Lepekhina, E. a; Thibau, I. J.; Pike, R. D.; Li, X.; Killarney, J. P.; Patterson, H. H. Copper(I) Thiocyanate-Amine Networks: Synthesis, Structure, and Luminescence Behavior. *Inorg. Chem.* **2011**, *50* (15), 7239–7249.

(9) Jung, M.; Kim, C.; Jeon, J.; Yang, S.; Seo, J. Thermal Stability of CuSCN Hole Conductor-Based Perovskite Solar Cells. *ChemSusChem* **2016**, *9*, 2592–2596.

(10) Liu, J.; Pathak, S. K.; Sakai, N.; Sheng, R.; Bai, S.; Wang, Z.; Snaith, H. J. Identification and Mitigation of a Critical Interfacial Instability in Perovskite Solar Cells Employing Copper Thiocyanate Hole-Transporter. *Adv. Mater. Interfaces* **2016**, *3*, 1600571.

(11) Chappaz-Gillot, C.; Berson, S.; Salazar, R.; Lechêne, B.; Aldakov, D.; Delaye, V.; Guillerez, S.; Ivanova, V. Polymer Solar Cells with Electrodeposited CuSCN Nanowires as New Efficient Hole Transporting Layer. *Sol. Energy Mater. Sol. Cells* **2014**, *120*, 163–167.

(12) Yaacobi-Gross, N.; Treat, N. D.; Pattanasattayavong, P.; Faber, H.; Perumal, A. K.; Stingelin, N.; Bradley, D. D. C.; Stavrinou, P. N.; Heeney, M.; Anthopoulos, T. D. High-Efficiency Organic Photovoltaic Cells Based on the Solution-Processable Hole Transporting Interlayer Copper Thiocyanate (CuSCN) as a Replacement for PEDOT:PSS. *Adv. Energy Mater.* **2015**, *5*, 1401529.

(13) Chaudhary, N.; Chaudhary, R.; Kesari, J. P.; Patra, A.; Chand, S. Copper Thiocyanate (CuSCN): An Efficient Solution-Processable Hole Transporting Layer In Organic Solar Cells. *J. Mater. Chem. C* **2015**, *3*, 11886–11892.

(14) Mishra, A.; Rana, T.; Looser, A.; Stolte, M.; Würthner, F.; Bäuerle, P.; Sharma, G. D.

High Performance A–D–A Oligothiophene-Based Organic Solar Cells Employing Two-Step Annealing and Solution-Processable Copper Thiocyanate (CuSCN) as an Interfacial Hole Transporting Layer. *J. Mater. Chem. A* **2016**, *4*, 17344–17353.

(15) Chavhan, S. D.; Miguel, O.; Grande, H.-J.; Gonzalez-Pedro, V.; Sanchez, R. S.; Barea, E. M.; Mora-Sero, I.; Tena-Zaera, R. Organo-Metal Halide Perovskite-Based Solar Cells with CuSCN as the Inorganic Hole Selective Contact. *J. Mater. Chem. A* **2014**, *2*, 12754–12760.

(16) Ito, S.; Tanaka, S.; Nishino, H. Lead-Halide Perovskite Solar Cells by CH3NH3I - Dripping on PbI2-CH3NH3I-DMSO Precursor Layer for Planar and Porous Structures Using CuSCN Hole Transporting Material. *J. Phys. Chem. Lett.* **2015**, *6*, 881–886.

(17) Zhao, K.; Munir, R.; Yan, B.; Yang, Y.; Kim, T.; Amassian, A. Solution-Processed Inorganic copper(I) Thiocyanate (CuSCN) Hole Transporting Layers for Efficient P–i–n Perovskite Solar Cells. *J. Mater. Chem. A* **2015**, *3*, 20554–20559.

(18) Jung, J. W.; Chueh, C.-C.; Jen, A. K.-Y. High-Performance Semitransparent Perovskite Solar Cells with 10% Power Conversion Efficiency and 25% Average Visible Transmittance Based on Transparent CuSCN as the Hole-Transporting Material. *Adv. Energy Mater.* **2015**, *5*, 1500486.

(19) Arora, N.; Dar, M. I.; Hinderhofer, A.; Pellet, N.; Schreiber, F.; Zakeeruddin, S. M.; Grätzel, M. Perovskite Solar Cells with CuSCN Hole Extraction Layers Yield Stabilized Efficiencies Greater than 20 %. *Science* **2017**.

(20) Subbiah, A. S.; Halder, A.; Ghosh, S.; Mahuli, N.; Hodes, G.; Sarkar, S. K. Inorganic

Hole Conducting Layers for Perovskite-Based Solar Cells. *J. Phys. Chem. Lett.* **2014**, *5* (10), 1748–1753.

(21) O'Regan, B. C.; Schwartz, D. T. Efficient Photo-Hole Injection from Adsorbed Cyanine Dyes into Electrodeposited Copper(1) Thiocyanate Thin Films. *Chem. Mater.* **1995**, *7*, 1349–1354.

(22) O'Regan, B. C.; Schwartz, D. T.; Zakeeruddin, S. M.; Grätzel, M. Electrodeposited Nanocomposite N-P Heterojunctions for Solid-State Dye-Sensitized Photovoltaics. *Adv. Mater.* **2000**, *12* (17), 1263–1267.

(23) Kumara, G. R. R. A.; Konno, A.; Senadeera, G. K. R.; Jayaweera, P. V. V.; De Silva, D. B. R. A.; Tennakone, K. Dye-Sensitized Solar Cell with the Hole Collector P-CuSCN Deposited from a Solution in N-Propyl Sulphide. *Sol. Energy Mater. Sol. Cells* **2001**, *69*, 195–199.

(24) Yoshida, T.; Zhang, J.; Komatsu, D.; Sawatani, S.; Minoura, H.; Pauporté, T.; Lincot, D.; Oekermann, T.; Schlettwein, D.; Tada, H.; et al. Electrodeposition of Inorganic/organic Hybrid Thin Films. *Adv. Funct. Mater.* **2009**, *19* (1), 17–43.

(25) Iwamoto, T.; Ogawa, Y.; Sun, L.; White, M. S.; Glowacki, E. D.; Scharber, M. C.; Sariciftci, N. S.; Manseki, K.; Sugiura, T.; Yoshida, T. Electrochemical Self-Assembly of Nanostructured CuSCN/Rhodamine B Hybrid Thin Film and Its Dye-Sensitized Photocathodic Properties. *J. Phys. Chem. C* **2014**, *118* (30), 16581–16590.

(26) Chen, K. J.; Laurent, A. D.; Boucher, F.; Odobel, F.; Jacquemin, D. Determining the Most Promising Anchors for CuSCN: Ab Initio Insights towards P-Type DSSCs. *J. Mater.*

Chem. A **2016**, *4*, 2217–2227.

(27) Kamat, P. V. Quantum Dot Solar Cells. The Next Big Thing in Photovoltaics. *J. Phys. Chem. Lett.* **2013**, *4*, 908–918.

(28) Yu, J.; Wang, W.; Pan, Z.; Du, J.; Ren, Z.; Xue, W.; Zhong, X. Quantum Dot Sensitized Solar Cells with Efficiency over 12% Based on Tetraethyl Orthosilicate Additive in Polysulfide Electrolyte. *J. Mater. Chem. A* **2017**, *5* (27), 14124–14133.

(29) Kamat, P. V.; Christians, J. A.; Radich, J. G. Quantum Dot Solar Cells: Hole Transfer as a Limiting Factor in Boosting the Photoconversion Efficiency. *Langmuir* **2014**, *30* (20), 5716–5725.

(30) Abdellah, M.; Marschan, R.; Žídek, K.; Messing, M. E.; Abdelwahab, A.; Chabera, P.; Zheng, K.; Pullerits, T. Hole Trapping: The Critical Factor for Quantum Dot Sensitized Solar Cell Performance. *J. Phys. Chem. C* **2014**, *118*, 25802–25808.

(31) Odobel, F.; Pellegrin, Y.; Gibson, E. A.; Hagfeldt, A.; Smeigh, A. L.; Hammarström, L. Recent Advances and Future Directions to Optimize the Performances of P-Type Dye-Sensitized Solar Cells. *Coord. Chem. Rev.* **2012**, *256* (21–22), 2414–2423.

(32) Aldakov, D.; Lefrançois, A.; Reiss, P. Ternary and Quaternary Metal Chalcogenide Nanocrystals: Synthesis, Properties and Applications. *J. Mater. Chem. C* **2013**, *1* (24), 3756–3776.

(33) Sandroni, M.; Wegner, K. D.; Aldakov, D.; Reiss, P. Prospects of Chalcopyrite-Type Nanocrystals for Energy Applications. *ACS Energy Lett.* **2017**, *2*, 1076–1088.

(34) Park, M.-A.; Lee, S.-Y.; Kim, J.-H.; Kang, S.-H.; Kim, H.; Choi, C.-J.; Ahn, K.-S. CdSe

Quantum Dot-Sensitized, Nanoporous P-Type NiO Photocathodes for Quantum Dot-Sensitized Solar Cells. *Mol. Cryst. Liq. Cryst.* **2014**, *598* (1), 154–162.

(35) Raissi, M.; Pellegrin, Y.; Jobic, S.; Boujtita, M.; Odobel, F. Infra-Red Photoresponse of Mesoscopic NiO-Based Solar Cells Sensitized with PbS Quantum Dot. *Sci. Rep.* **2016**, *6* (April), 24908.

(36) Barceló, I.; Guillen, E.; Lana-Villarreal, T.; Gomez, R. Preparation and Characterization of Nickel Oxide Photocathodes Sensitized with Colloidal Cadmium Selenide Quantum Dots. *J. Phys. Chem. C* **2013**, *117*, 22509–22517.

(37) Li, X.; Chen, R.; Sui, H.; Yuan, X.; Li, M.; Yang, K.; Li, L.; Zhang, W.; Zhang, Y. Photoelectrochemical Properties of CdSe Quantum Dot Sensitized P-Type Flower-like NiO Solar Cells with Different Deposition Layer. *Mater. Res. Bull.* **2016**, *84*, 212–217.

(38) Park, J.; Sajjad, M. T.; Jouneau, P.-H.; Ruseckas, A.; Faure-Vincent, J.; Samuel, I. D. W.; Reiss, P.; Aldakov, D. Efficient Eco-Friendly Inverted Quantum Dot Sensitized Solar Cells. *J. Mater. Chem. A* **2016**, *4*, 827–837.

(39) Mao, Y.-Q.; Zhou, Z.-J.; Ling, T.; Du, X.-W. P-Type CoO Nanowire Arrays and Their Application in Quantum Dot-Sensitized Solar Cells. *RSC Adv.* **2013**, *3* (4), 1217.

(40) Zhao, C.; Zou, X.; He, S. CdTeO 3 Deposited Mesoporous NiO Photocathode for a Solar Cell. *J. Nanomater.* **2014**, *2014*, 372381.

(41) Gertman, R.; Harush, A.; Visoly-Fisher, I. Nanostructured Photocathodes for Infrared Photodetectors and Photovoltaics. *J. Phys. Chem. C* **2015**, *119* (4), 1683–1689.

(42) Gan, X.; Liu, K.; Du, X.; Guo, L.; Liu, H. Bath Temperature and Deposition Potential

Dependences of CuSCN Nanorod Arrays Prepared by Electrochemical Deposition. *J. Mater. Sci.* **2015**, *50*, 7866–7874.

(43) Chappaz-Gillot, C.; Salazar, R.; Berson, S.; Ivanova, V. Room Temperature Template-Free Electrodeposition of CuSCN Nanowires. *Electrochem. commun.* **2012**, *24*, 1–4.

(44) Sanchez, S.; Chappaz-Gillot, C.; Salazar, R.; Muguerra, H.; Arbaoui, E.; Berson, S.; Lévy-Clément, C.; Ivanova, V. Comparative Study of ZnO and CuSCN Semiconducting Nanowire Electrodeposition on Different Substrates. *J. Solid State Electrochem.* **2012**, *17* (2), 391–398.

(45) Aldakov, D.; Chappaz-Gillot, C.; Salazar, R.; Delaye, V.; Welsby, K. A.; Ivanova, V.; Dunstan, P. R. Properties of Electrodeposited CuSCN 2D Layers and Nanowires Influenced by Their Mixed Domain Structure. *J. Phys. Chem. C* **2014**, *118*, 16095–16103.

(46) Mora-Seró, I.; Giménez, S.; Fabregat-Santiago, F.; Gomez, R. G.; Shen, Q.; Toyoda, T.; Bisquert, J. Recombination in Quantum Dot Sensitized Solar Cells. *Acc. Chem. Res.* **2009**, *42* (11), 1848–1857.

(47) Kim, J.; Yang, J.; Yu, J. H.; Baek, W.; Lee, C.; Son, H. J.; Hyeon, T.; Ko, M. J. Highly Efficient Copper Indium Selenide Quantum Dot Solar Cells: Suppression of Carrier Recombination by Controlled ZnS Overlayers. *ACS Nano* **2015**, *9* (11), 11286–11295.

(48) Zhao, K.; Pan, Z.; Zhong, X. Charge Recombination Control for High Efficiency Quantum Dot Sensitized Solar Cells. *J. Phys. Chem. Lett.* **2016**, *7*, 406–417.

(49) Wen, L.; Zhou, M.; Wang, C.; Mi, Y.; Lei, Y. Nanoengineering Energy Conversion and Storage Devices via Atomic Layer Deposition. *Adv. Energy Mater.* **2016**, *6*, 1600468.

(50) Luan, C.; Vaneski, A.; Susha, A. S.; Xu, X.; Wang, H.-E.; Chen, X.; Xu, J.; Zhang, W.; Lee, C.-S.; Rogach, A. L.; et al. Facile Solution Growth of Vertically Aligned ZnO Nanorods Sensitized with Aqueous CdS and CdSe Quantum Dots for Photovoltaic Applications. *Nanoscale Res. Lett.* **2011**, *6* (1), 340.

(51) Roelofs, K. E.; Brennan, T. P.; Dominguez, J. C.; Bailie, C. D.; Margulis, G. Y.; Hoke, E. T.; Mcgehee, M. D.; Bent, S. F. Effect of Al2O3 Recombination Barrier Layers Deposited by Atomic Layer Deposition in Solid-State CdS Quantum Dot-Sensitized Solar Cells. *J. Phys. Chem. C* **2013**, *117*, 5584–5592.

(52) Zeng, M.; Peng, X.; Liao, J.; Wang, G.; Li, Y.; Li, J.; Qin, Y.; Wilson, J.; Song, A.; Lin, S. Enhanced Photoelectrochemical Performance of Quantum Dot-Sensitized TiO2 Nanotube Arrays with Al2O3 Overcoating by Atomic Layer Deposition. *Phys. Chem. Chem. Phys.* **2016**, *18*, 17404–17413.

(53) McDaniel, H.; Fuke, N.; Makarov, N. S.; Pietryga, J. M.; Klimov, V. I. An Integrated Approach to Realizing High-Performance Liquid-Junction Quantum Dot Sensitized Solar Cells. *Nat. Commun.* **2013**, *4*, 2887.

(54) Evangelista, R. M.; Makuta, S.; Yonezu, S.; Andrews, J.; Tachibana, Y. Semiconductor Quantum Dot Sensitized Solar Cells Based on Ferricyanide/Ferrocyanide Redox Electrolyte Reaching an Open Circuit Photovoltage of 0.8 V. *ACS Appl. Mater. Interfaces* **2016**, *8* (22), 13957–13965.

(55) Pattanasattayavong, P.; Promarak, V.; Anthopoulos, T. D. Electronic Properties of Copper(I) Thiocyanate (CuSCN). *Adv. Electron. Mater.* **2017**, *3* (I), 1600378.

(56) Treat, N. D.; Yaacobi-Gross, N.; Faber, H.; Perumal, A. K.; Bradley, D. D. C.; Stingelin, N.; Anthopoulos, T. D. Copper Thiocyanate: An Attractive Hole Transport/extraction Layer for Use in Organic Photovoltaic Cells. *Appl. Phys. Lett.* **2015**, *107* (1), 13301.

(57) Aldakov, D.; Sajjad, M. T.; Ivanova, V.; Bansal, A. K.; Park, J.; Reiss, P.; Samuel, I. D. W. Mercaptophosphonic Acids as Efficient Linkers in Quantum Dot Sensitized Solar Cells. *J. Mater. Chem. A* **2015**, *3* (37), 19050–19060.

(58) Rhee, J. H.; Lee, Y. H.; Bera, P.; Seok, S. I. Cu2S-Deposited Mesoporous NiO Photocathode for a Solar Cell. *Chem. Phys. Lett.* **2009**, *477* (4–6), 345–348.

(59) Radich, J. G.; Peeples, N. R.; Santra, P. K.; Kamat, P. V. Charge Transfer Mediation Through CuxS. The Hole Story of CdSe in Polysulfide. *J. Phys. Chem. C* **2014**, *118*, 16463–16471.

(60) Makarov, N. S.; Mcdaniel, H.; Fuke, N.; Robel, I.; Klimov, V. I. Photocharging Artifacts in Measurements of Electron Transfer in Quantum-Dot-Sensitized Mesoporous Titania Films. *J. Phys. Chem. Lett.* **2014**, *5*, 111–118.

(61) Raissi, M.; Sajjad, M. T.; Pellegrin, Y.; Roland, T. J.; Jobic, S.; Boujtita, M.; Ruseckas, A.; Samuel, I. D. W.; Odobel, F. Size Dependence of Efficiency of PbS Quantum Dots in NiO-Based Dye Sensitised Solar Cells and Mechanistic Charge Transfer Investigation. *Nanoscale* **2017**, *9*, 15566–15575.

(62) Gibson, E. A.; Smeigh, A. L.; Pleux, L. Le; Hammarstrom, L.; Odobel, F.; Boschloo, G.; Hagfeldt, A.; Hammarström, L.; Odobel, F.; Boschloo, G.; et al. Cobalt Polypyridyl-Based Electrolytes for P-Type Dye-Sensitized Solar Cells. *J. Phys. Chem. C* **2011**, *115*, 9772–

9779.

(63) Gaboriau, D.; Boniface, M.; Valero, A.; Aldakov, D.; Brousse, T.; Gentile, P.; Sadki, S. ALD Alumina Passivated Silicon Nanowires: Probing the Transition from Electrochemical Double Layer Capacitor to Electrolytic Capacitors. *ACS Appl. Mater. Interfaces* **2017**, *9* (15), 13761–13769.

(64) Black, F. A.; Wood, C. J.; Ngwerume, S.; Summers, G. H.; Clark, I. P.; Towrie, M.; Camp, J. E.; Gibson, E. A. Charge-Transfer Dynamics at the Dye–semiconductor Interface of Photocathodes for Solar Energy Applications. *Faraday Discuss.* **2017**, *198*, 449–461.

(65) Pham, T. T. T.; Saha, S. K.; Provost, D.; Farré, Y.; Raissi, M.; Pellegrin, Y.; Blart, E.; Vedraine, S.; Ratier, B.; Aldakov, D.; et al. Toward Efficient Solid-State P-Type Dye-Sensitized Solar Cells: The Dye Matters. *J. Phys. Chem. C* **2017**, *121*, 129–139.

TOC Graphic

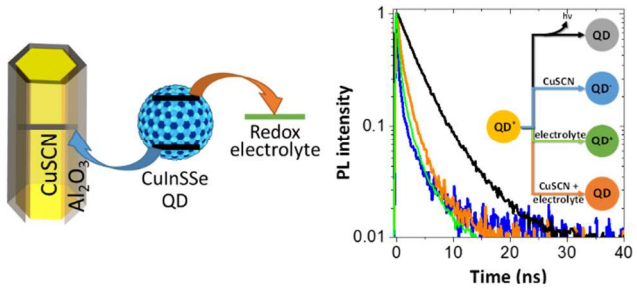
CuSCN
Al_2O_3
CuInSSe
QD
Redox
electrolyte
PL intensity
1
0.1
0.01
0
10
20
30
40
Time (ns)
hν
QD
CuSCN
QD⁻
QD⁺
electrolyte
QD⁺
CuSCN +
electrolyte
QD